PHILOSOPHICAL TRANSACTIONS OF THE ROYAL SOCIETY B BIOLOGICAL SCIENCES

Southern Ocean Sea-Ice Distributions and Extents [and Discussion]

Claire L. Parkinson, J. C. Moore, B. Stonehouse and G. De Q. Robin

Phil. Trans. R. Soc. Lond. B 1992 **338**, 243-250
doi: 10.1098/rstb.1992.0144

Southern Ocean sea-ice distributions and extents

CLAIRE L. PARKINSON

Oceans and Ice Branch/Code 971, NASA Goddard Space Flight Center, Greenbelt, Maryland 20771, U.S.A.

SUMMARY

Southern Ocean sea-ice coverage undergoes a large seasonal cycle, with a nearly fivefold increase in areal ice extents from the minimum in February to the maximum in September, and significant interannual variations. Results presented here show in a variety of forms some of the variability that occurred in Southern Ocean sea-ice distributions and extents over the 1970s and 1980s. Interannual variability is examined by identifying changes in three measures: sea-ice extents, sea-ice distributions, and the length of the sea-ice season. Regarding these three: (i) Maximum ice extents varied by approximately 12%, decreasing during the mid-1970s, followed by increases over the next few years and a levelling off for much of the 1980s. (ii) The area of interannual variability in monthly average sea-ice distributions in summer far exceeds the summertime area of consistent ice coverage, in sharp contrast to the wintertime situation, when the area of consistent ice coverage is considerably larger. In winter, the ice-distribution variability is largely confined to two regions: a relatively narrow outer band (generally 2–5° of latitude) surrounding the region of consistent ice coverage, and, for the mid-1970s, the region of an occasional large open water area within the ice pack of the Weddell Sea, termed the Weddell polynya. The Weddell and other polynyas within the ice cover allow intensified heat, mass, and momentum exchanges between ocean and atmosphere, thereby affecting regional oceanic and atmospheric circulations. (iii) The length of the sea-ice season, calculated for the years 1979–1986, with satellite passive-microwave data coverage through all months of the year, showed increases over that period in the Ross Sea but decreases in the Weddell and Bellingshausen seas. In both cases it appears, through comparisons with data from 1973–1976, that the 1979–1986 changes more likely reflect a fluctuating behaviour of the ice cover than a long-term trend. The changes in the ice cover have influences not only on the ocean and the atmosphere but on aquatic plant and animal life as well.

1. INTRODUCTION

Global climate is well known to be an integrally coupled system (Cubasch & Cess 1990). Many components, including the stratosphere, troposphere, upper ocean, deeper ocean, sea ice, land ice, vegetation, and soil moisture, are bound together to various extents and at various timescales. Furthermore, all large spatial regions both are affected by and affect other regions in the system. In the case of the Antarctic, the highly negative radiation balance, with more radiation emitted than absorbed, is countered by the strong net inflow of heat energy from the north through both ocean currents and atmospheric winds (Barry & Chorley 1985).

Sea ice affects many aspects of the Antarctic environment. Because of its high albedo relative to that of seawater, sea ice lessens the amount of solar radiation absorbed at the ocean surface. Because of the inefficiency of molecular conduction through the ice as a heat transfer mechanism and the lower surface temperature of the ice than of the ocean, sea ice reduces the sensible heat flux from the ocean to the atmosphere. This effect is especially strong in winter, when the ocean–atmosphere temperature gradient is large. Because of greater evaporation rates from water than sublimation rates from adjacent ice floes, sea ice also lessens the mass flux of water vapour to the atmosphere; and because of the momentum consumed in ice floe motions and interactions, sea ice lessens the oppositely directed transfer of momentum from the atmosphere to the water. Furthermore, sea ice has significant qualitative as well as quantitative impacts. For instance, because sea ice rejects salt to the underlying water as it forms and ages, sea ice influences the density of the water and thereby the tendency toward convective overturning. The salt rejected from sea ice sometimes precipitates a deepening of the local oceanic mixed layer, and this occasionally leads to the formation of Antarctic bottom water. Antarctic bottom water in turn affects the bottom water circulation throughout the global oceans. The presence of sea ice also affects marine life, providing a surface for some animals to live on and affecting the light and heat transmission to the organisms in the underlying water. Quantitative details on various impacts of sea ice on the surrounding environment can be found in Grenfell & Maykut (1977) for the albedo effect, in Maykut (1982) for the reduction of sensible and latent heat transfers, and in Warren (1981) & Killworth (1983) for the effect on deep convection.

The importance of sea ice to the other elements of the climate system and to the biosphere is one primary reason for desiring an accurate record of sea-ice

Phil. Trans. R. Soc. Lond. B (1992) **338,** 243–250
Printed in Great Britain

locations. Another reason beyond the obvious practical one of assisting ships operating in high-latitude waters is the determination of what if any climate changes are occurring in the ice cover and how these changes might be connected to other changes in the climate system.

Historically, knowledge of the Southern Ocean sea-ice cover has been severely data-limited, due in large part to the remoteness of the region and the harshness of the polar conditions. Fortunately the availability of data has improved markedly over the past 20 years, as satellite technology has allowed remotely based data collection at a variety of temporal and spatial scales. Of particular importance to the understanding of the Southern Ocean ice cover have been satellite passive-microwave observations, which have allowed data coverage of the entire Southern Ocean to a spatial resolution of about 30–60 km and a temporal resolution of every few days. Satellite passive-microwave data have permitted a detailed description of the seasonally and interannually changing distributions of the sea ice of the Southern Ocean for much of the period since the start of 1973. In this paper the longest satellite passive-microwave record to date, the 8.8-year record from the Scanning Multichannel Microwave Radiometer (SMMR) on the Nimbus 7 satellite, is used to analyse Southern Ocean sea-ice distributions and extents and their changes over the course of the SMMR record. At the end of the paper these changes are compared with the earlier, extensively analysed 4-year record for 1973–1976 from the Electrically Scanning Microwave Radiometer (ESMR) on board the Nimbus 5 satellite.

2. DATA

The main data source for this study is a set of monthly average Southern Ocean sea-ice concentrations (percent areal coverages of sea ice) derived from the data of the Nimbus 7 SMMR, a passive-microwave instrument that operated, generally on an every-other-day basis, for most of the period from the launch of the Nimbus 7 satellite on 24 October, 1978 until the turning off of the SMMR's scanning mechanism on 20 August, 1987. The resulting 8.8-year record far exceeds in length both the anticipated life span of the SMMR and the record length from any previous microwave sensor. By using the SMMR record exclusively for the figures in this paper, the ice extents and distributions in the Southern Ocean over an 8.8-year period can be summarized while avoiding the many complications arising from inconsistencies among different instruments.

The Nimbus 7 SMMR was a ten-channel radiometer receiving horizontally and vertically polarized data at each of five wavelengths between 0.81 cm and 4.5 cm. It operated with a conical scan that maintained a constant incidence angle of 50° and a swath width of 780 km. Its characteristics in combination with the Nimbus 7 orbit allowed routine data coverage everywhere equatorward of about 84.6° latitude, including the entire Southern Ocean. Further details about the SMMR can be found in Gloersen & Barath (1977).

The algorithm used to derive sea ice concentrations from the SMMR data employs three of the ten SMMR channels and is based on (i) the contrast between the microwave emissions of sea ice and open water, and (ii) the fact that undesired temperature effects can be sharply reduced through use of two radiance ratios, the polarization and the gradient ratio. The three channels employed are those receiving horizontally polarized radiation at a wavelength of 1.7 cm and vertically polarized radiation at wavelengths of 0.81 cm and 1.7 cm. The polarization ratio PR and gradient ratio GR are calculated from these data as:

$$PR = \frac{TB\,(V, 1.7\text{ cm}) - TB\,(H, 1.7\text{ cm})}{TB\,(V, 1.7\text{ cm}) + TB\,(H, 1.7\text{ cm})} \quad (1)$$

and

$$GR = \frac{TB\,(V, 0.81\text{ cm}) - TB\,(V, 1.7\text{ cm})}{TB\,(V, 0.81\text{ cm}) + TB\,(V, 1.7\text{ cm})}, \quad (2)$$

where $TB\,(V,\lambda)$ and $TB\,(H,\lambda)$ are the brightness temperatures (in Kelvins) at wavelength λ for vertically and horizontally polarized radiation, respectively. The PR values for water significantly exceed those for ice, whereas different ice types have distinctly different GR values. The contrasts allow the calculation of ice concentrations, and secondarily the calculation of the concentrations of two separate ice types, from the PR and GR values. The algorithm for deriving the ice concentrations was first developed by Cavalieri *et al.* (1984) and is described in detail, in a somewhat modified form, in Gloersen *et al.* (1992). The accuracy of the derived ice concentrations is estimated to be ± 7%, based on quantitative comparisons with Landsat imagery (Gloersen *et al.* 1992). The spatial resolution of the concentrations is approximately 55 km, as is the spatial resolution of the radiances from the 1.7 cm channels. The 0.81 cm channel has a somewhat finer spatial resolution of approximately 30 km. The ice concentrations are gridded to grid elements of approximately 25 km × 25 km.

The digital data set of SMMR-derived sea-ice concentrations is available on CD-ROMs through the National Snow and Ice Data Center (NSIDC) in Boulder, Colorado. Colour images of the derived sea-ice concentrations for each polar region for each month from November 1978 through August 1987 are included in Gloersen *et al.* (1992).

3. AVERAGE SEASONAL CYCLE OF SOUTHERN OCEAN SEA ICE, 1978–1987

The Nimbus 7 SMMR data are used in this and the following section to describe major aspects of Southern Ocean sea-ice variability, starting here with the most basic of all, the seasonal cycle, and proceeding in the next section to three measures of interannual variability. The seasonal cycle is described both from the perspective of sea-ice extents, defined as the area of the ocean covered by sea ice with concentration (in the 25 km × 25 km grid elements) of at least 15%, and

PHILOSOPHICAL TRANSACTIONS OF THE ROYAL SOCIETY B BIOLOGICAL SCIENCES

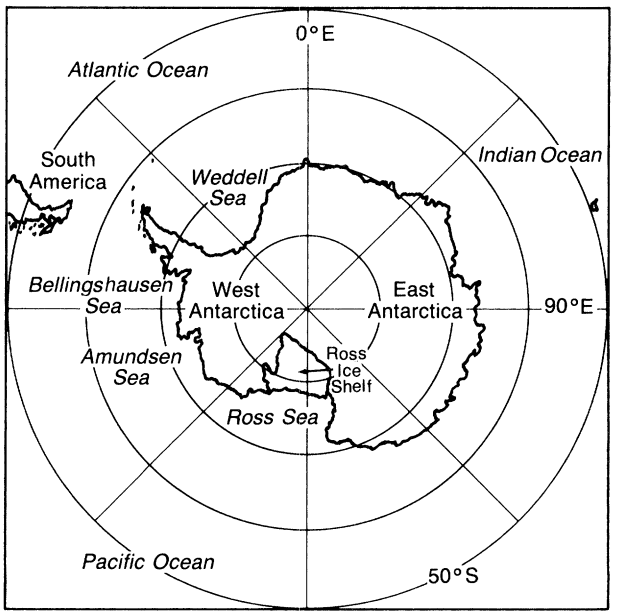

Figure 1. Location map.

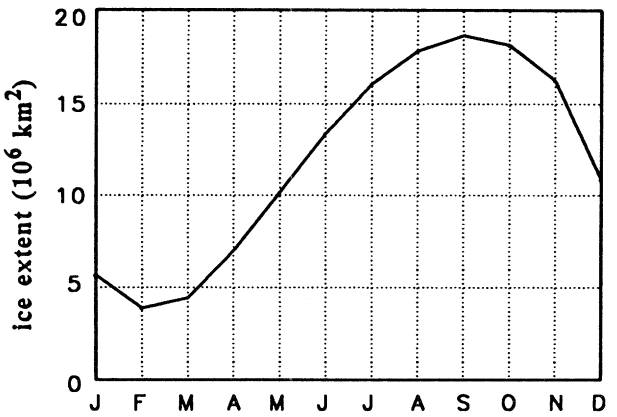

Figure 2. Average seasonal cycle of monthly average Southern Ocean sea-ice extents over the period with full-month data coverage by the Nimbus 7 SMMR, November 1978 through July 1987. Ice extents are calculated from the passive-microwave SMMR data as the areal coverage of the Southern Ocean with ice concentrations exceeding 15%.

from the perspective of the spatial distributions of the ice, again using a 15% ice concentration cutoff for the ice edge. A location map is provided in figure 1.

(*a*) *Sea-ice extents*

Over the course of the SMMR data record, monthly average sea-ice extents in the Southern Ocean experienced an average seasonal cycle that had a minimum of 3.9×10^6 km^2 in February, followed by a slow growth from February to March, a faster and near uniform growth from March to July, a continued but slightly less rapid growth from July to August, and a further slight slowing of the growth from August to September (figure 2). The average ice extents reached a maximum of 18.6×10^6 km^2 in September, then decreased slightly from September to October, more rapidly from October to November, and most rapidly from November to January, prior to a considerable slowing of the decay from January to the ice extent minimum in February (figure 2). Although the magnitudes of the ice extents varied from year to year, as detailed in the next section, there was considerable consistency in the general shape and timing of the seasonal cycle. In particular, in each year of the data set minimum ice extent occurred in February and maximum ice extent occurred in September (Gloersen *et al.* 1992).

The seasonal asymmetry apparent in figure 2, with the spring–summer decay (September to February) proceeding more rapidly than the autumn–winter growth (February to September), has been noted previously for other years and contrasted with the more symmetric growth–decay cycle typical of the Arctic (e.g. Gordon 1981; Parkinson *et al.* 1987). The more rapid decay of the Antarctic ice likely results from a significantly greater upwelling of relatively warm deep water in the Antarctic than in the Arctic (Gordon 1981).

(*b*) *Sea-ice distributions*

Spatially, the Southern Ocean ice at the summer minimum is confined largely to the western Weddell Sea, the southern Bellingshausen and Amundsen seas, and the southeastern Ross Sea, although a narrow fringe of ice also exists around most of the rest of the continent (figure 3). Expansion of the ice from February to March is most noticeable in the Ross Sea and from March to April in the Ross and Weddell Seas. Expansion then continues outward at all longitudes, until by September the ice edge has reached equatorward to 54°–65°S. At the September maximum, the ice edge is furthest equatorward in the far eastern Weddell Sea, at about 15°E, where it reaches 54°S, and furthest poleward in the western Bellingshausen Sea, where it is located at 65°S (figure 3). As the ice cover decays from September to February, two major exceptions to the generally north-to-south retreat are (i) the opening of the polynya (open water region) off the Ross Ice Shelf in December, with the decay of the ice cover then proceeding outward from the polynya as well as inward from the outer ice edge, and (ii) the east-to-west retreat of the ice edge in the Weddell Sea from December to February (figure 3). Both anomalies are probably caused by a combination of atmospheric and oceanographic factors. In the case of the Ross Sea polynya, Jacobs & Comiso (1989) have examined the SMMR ice data in conjunction with atmospheric, oceanographic, and bathymetric data and have concluded that the formation and maintenance of the polynya are strongly influenced by the upwelling of relatively warm, high-salinity water along the continental slope (trending from about 75°S off the eastern portion of the ice shelf to about 71°S off the western portion of the ice shelf) and by atmospheric forcing from strong winds off the continent, helping to advect newly formed ice northward.

PHILOSOPHICAL TRANSACTIONS OF THE ROYAL SOCIETY B BIOLOGICAL SCIENCES

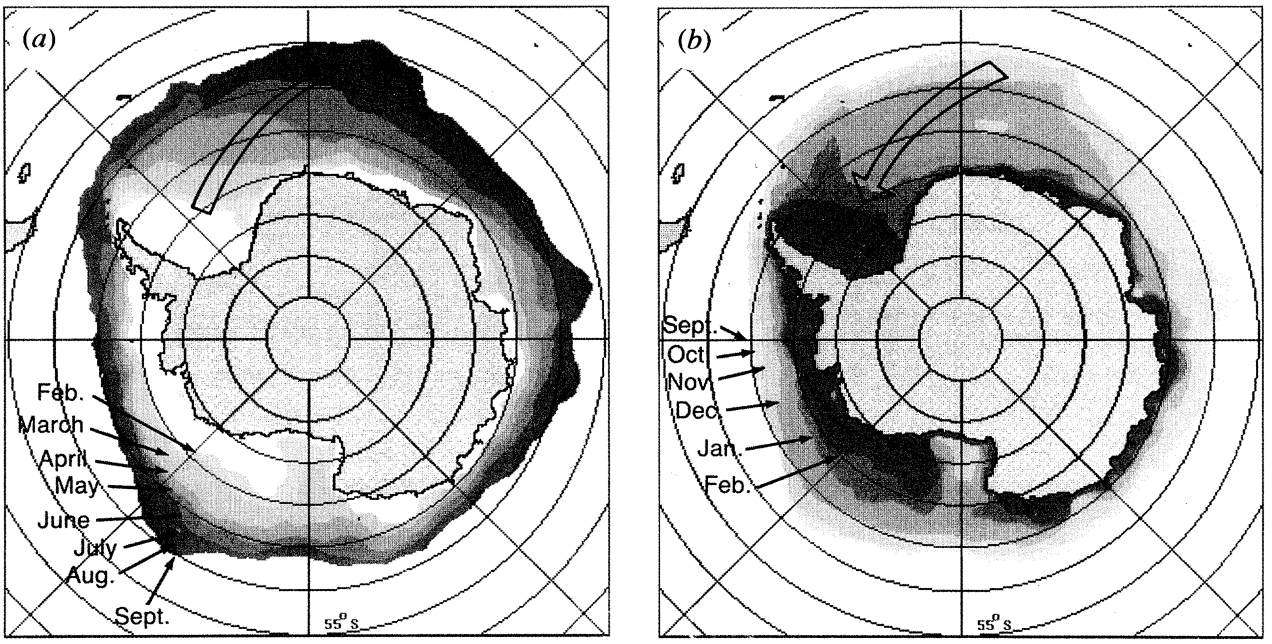

Figure 3. Average seasonal cycle of the monthly average spatial distributions of sea ice in the Southern Ocean over the period of the Nimbus 7 SMMR record, showing (*a*) the ice distributions during the growth period, February–September, and (*b*) the ice distributions during the decay period, September–February.

4. INTERANNUAL VARIABILITY IN SOUTHERN OCEAN SEA ICE, 1978–1987

The interannual variability experienced by Southern Ocean sea ice over the course of the SMMR satellite record is illustrated here by three measures. Of these, the first considers changes in the overall areal extent of the Southern Ocean ice, the second considers the spatial range experienced in the monthly average Southern Ocean ice distributions, illustrated with the months of February, September, and December, and the third considers trends in the length of the Southern Ocean sea-ice season. The first measure has been examined in several previous studies, for various time periods; the second was first examined, for a different

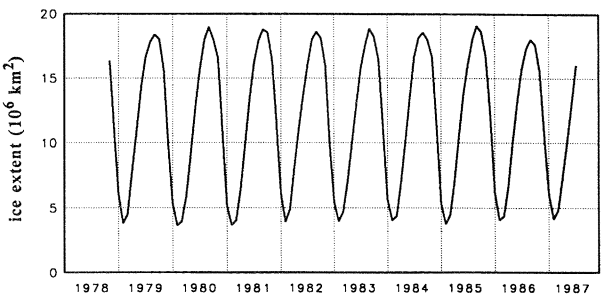

Figure 4. Monthly average Southern Ocean sea-ice extents for November 1978 through July 1987, calculated from the data of the Nimbus 7 SMMR. The vertical grid lines occur at January of each year.

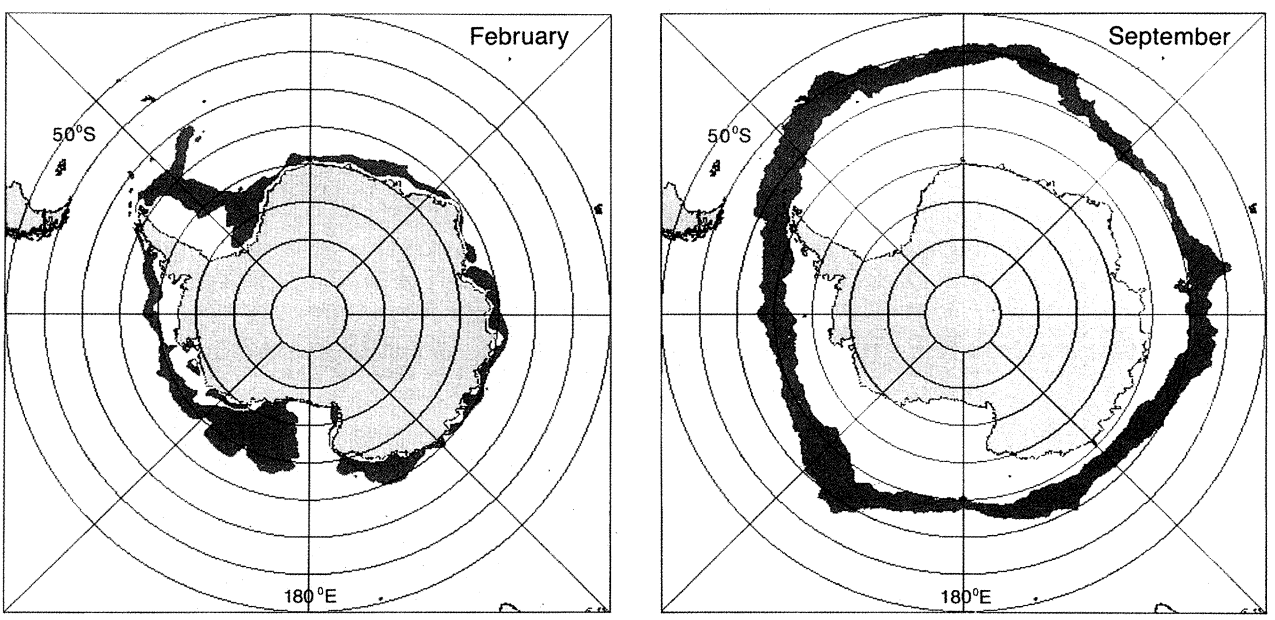

Figure 5. For description see opposite.

set of years, in a study just published (Parkinson 1992); and the third is here appearing for the first time.

(*a*) *Sea-ice extents*

When monthly average Southern Ocean sea-ice extents are plotted for the full SMMR record, no strong increasing or decreasing long-term trends are apparent (figure 4). Yearly maximum ice extents range from 18.0×10^6 km^2 in September 1986 to 19.1×10^6 km^2 in September 1985. Hence, although the lowest maximum was in the last full year of the data set, the highest maximum was in the immediately preceding year. Furthermore, the second lowest maximum was in the first full year of the data set (1979), and the second highest maximum was in the second full year (1980). Maximum monthly average ice extents thus show a mild interannual variability of about 6% over the course of the SMMR record, with the nature of this variability not being one of a long-term trend (figure 4). Regarding minimum ice extents, the range is from 3.6×10^6 km^2 in February 1980 to 4.1×10^6 km^2 in February 1987, yielding an interannual variability of 12%. Although there exists a slight suggestion of an overall upward trend in the minimum values, the increases are by no means uniform or monotonic (figure 4).

(*b*) *Sea-ice distributions*

Monthly maps have been generated showing both the locus of spatial variability in monthly average sea ice distributions over the course of the SMMR data set and the locus of consistent ice coverage over the

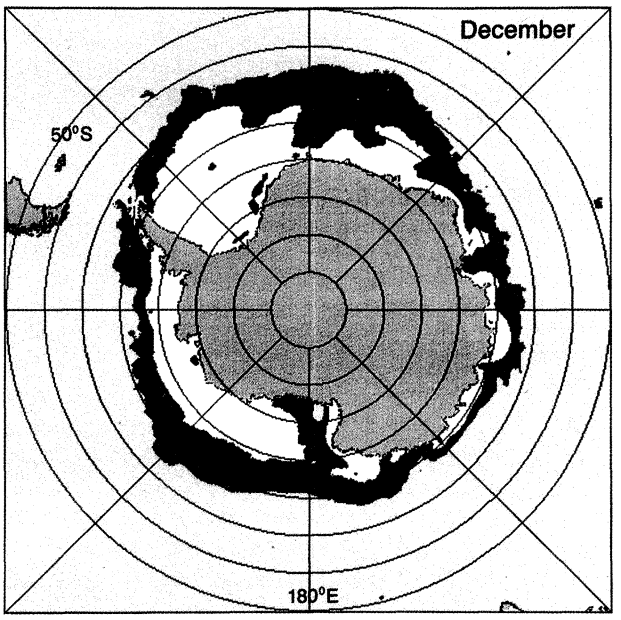

Figure 6. Same as figure 5 but for December.

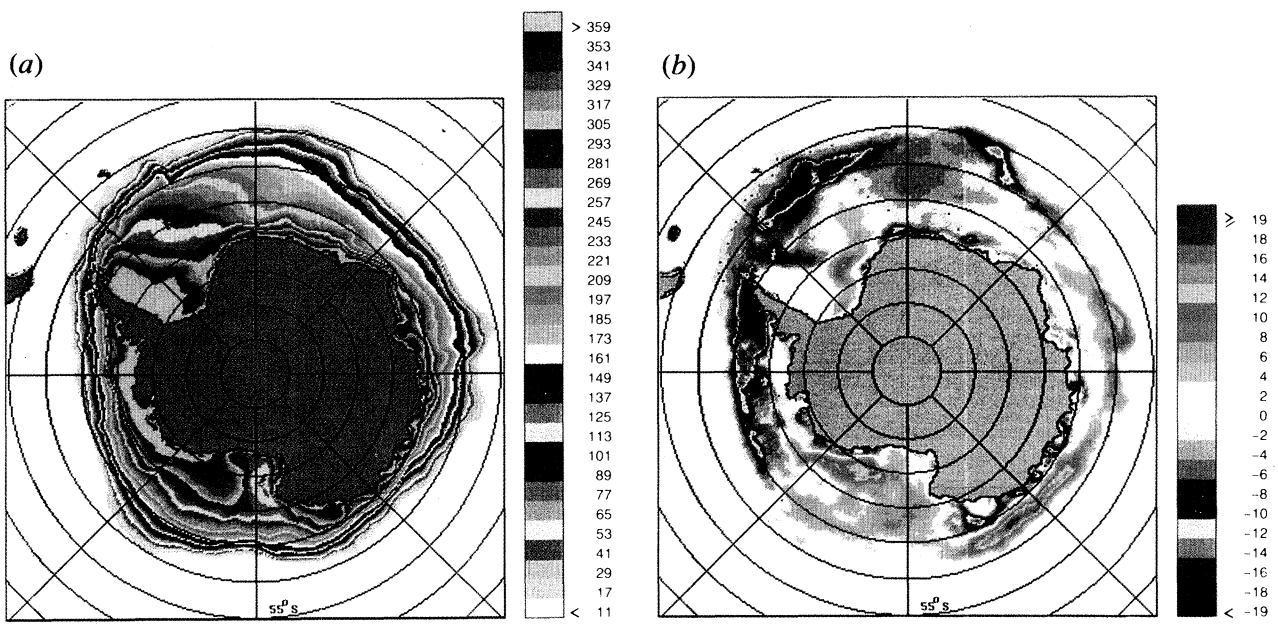

Figure 7. (*a*) Average length, in days, of the Southern Ocean sea-ice season, 1979–1986, as determined from the Nimbus 7 SMMR data, using an ice concentration cutoff of 15%. (*b*) Trends in the length of the Southern Ocean sea-ice season from 1979 to 1986, calculated as the slopes of the lines of least squares fit through the yearly values of the ice season lengths. The trends are given in units of days per year.

Figure 5. Locus of spatial variability in monthly average Southern Ocean sea-ice distributions over the years of the SMMR data set, for the months February and September. In each case, white indicates that the monthly average ice concentration for the given month was at least 15% for each year of the SMMR data set; green indicates that the monthly average ice concentration for the given month was at least 15% for some but not all years of the data set; and blue indicates that the monthly average ice concentration for the given month was not as high as 15% for any year of the data set.

PHILOSOPHICAL TRANSACTIONS OF THE ROYAL SOCIETY B BIOLOGICAL SCIENCES

same period. Figure 5 presents the results for February and September, the months of minimum and maximum ice coverage, respectively, and Figure 6 presents the results for December, within the period of rapid ice decay. (Similar monthly maps have been created for the combined ESMR/SMMR time period, although for an ice concentration cutoff of 30% instead of the 15% used here. The full set of 12 such maps can be found in Parkinson (1992).)

In February, the region of consistent ice coverage is confined largely to the western Weddell Sea and the southern Bellingshausen and Amundsen seas (figure 5). The region of occasional ice coverage is considerably larger and includes sizeable areas in the central Weddell Sea and especially the eastern Ross Sea as well as a more narrow fringe around the rest of the continent (figure 5).

In September, the region of consistent ice coverage completely surrounds Antarctica and extends a considerable distance outward from the continent at most longitudes (figure 5). The interannual variability in the September ice distributions is confined to an outer band around the entire ice edge, with the band width varying from under 1° latitude at about 60°E to 7° latitude at about 135°W (figure 5). In December, the outer band of variability is much broader at some longitudes, reaching 11° of latitude in the eastern Weddell Sea and 12° of latitude off the Ross Ice Shelf (figure 6). In December there are also scattered isolated regions of variability within the area of consistent ice coverage, indicating occasional polynya openings, and a region directly off the Ross Ice Shelf that is ice-free in each December (figure 6).

The variability maps in figures 5 and 6 can assist in various practical and climate-oriented considerations regarding the sea-ice cover. Specifically, they outline the regions in which ships can expect to encounter ice, and they provide concise maps for comparing against future sea-ice data sets. If future ice edges remain within the range of variability found over the SMMR years, justification of claims of climatic change in the ice cover distributions between the SMMR years and those future dates would be difficult. Thus regions and times exhibiting particularly high variability and very little area of consistent ice coverage, such as the eastern Ross Sea in February, would be poor choices for concentrating the search for future climate change in the sea-ice cover.

(*c*) *Trends in the length of the sea-ice season*

To obtain a spatial depiction of basic changes occurring in the Southern Ocean sea-ice coverages over the course of the SMMR record, a new variable, the length of the Southern Ocean sea-ice season, was calculated and examined for trends. Figure 7*a* presents a map of the average length of the sea-ice season, defined as the number of days with ice concentration exceeding 15%, over the course of the eight complete years of the SMMR record (1979–1986). The regions of perennial sea-ice coverage in the western Weddell and southern Bellingshausen and Amundsen seas are clearly delineated, as is the eastward pulse of ice growth (and westward decay) in the Weddell Sea and the westward pulse in the Ross Sea. Also apparent is the relatively short ice season (245–270 days) directly north of the Ross Ice Shelf, reflecting the consistently early opening of the ice cover in that region, described by Jacobs & Comiso (1989) and others.

Trends in the length of the ice season over the 1979–1986 period have been calculated as the slopes, at each grid square, of the least squares fits through the yearly season-length values. When mapped, these give a general indication of the spatial patterns of the overall direction of change over the course of the SMMR record (figure 7*b*). The overall trends were toward longer ice seasons in the Ross Sea and around much of East Antarctica, but toward shorter ice seasons in the Weddell and Bellingshausen seas (figure 7*b*). There is a strong spatial coherence in the results, and some of the patterns are suggestive of causal mechanisms. For instance, the tendency around much of East Antarctica for a shortening of the sea-ice season adjacent to the coast but a lengthening of the season further equatorward suggests the possibility of increased divergence, perhaps from increased wind flow from the continent, driving ice outward from the coastal regions, early in the melt season. This divergence would lengthen the season away from the coast, from the advective addition of ice, but would reduce ice concentrations near the coast, increasing the local oceanic absorption of solar radiation and thereby likely speeding the summertime disappearance of the coastal ice cover.

5. COMPARISONS WITH CONDITIONS IN THE MID-1970s

Prior to the 8.8-year SMMR record, the only several-year record of the full Southern Ocean ice cover with comparable detail was the 4-year record from the Nimbus 5 ESMR. The ESMR record for the Southern Ocean has been extensively analysed, most notably by Zwally *et al.* (1983*a*), and some comparisons between the ESMR results and the SMMR results shown here are relevant.

The most striking feature of the ESMR years that did not occur in the SMMR years was a large wintertime open water region in the eastern Weddell Sea, termed the Weddell polynya, that occurred in 1974, 1975, and 1976 (Carsey 1980; Zwally *et al.* 1983*a*; Comiso & Gordon 1987). Hence when maps such as those in figures 5 and 6 are created of the locus of spatial variability in Southern Ocean sea-ice distributions for the ESMR years instead of for the SMMR years, or for the ESMR and SMMR years combined, as was done by Parkinson (1992), the September map contains a prominent isolated region of variability in the eastern Weddell Sea (64–71°S; 23°W–14°E) in addition to the outer band of variability found during the SMMR years. This isolated region of variability is the reflection of the Weddell polynya and gives the appearance of a far more variable wintertime ice cover in the Weddell Sea in the mid-1970s than in the 1980s.

PHILOSOPHICAL TRANSACTIONS OF THE ROYAL SOCIETY B BIOLOGICAL SCIENCES

In the case of sea-ice extents, calculated values of yearly maximum ice extent for the Southern Ocean as a whole tended to be higher in the ESMR years, when they ranged from 19.0×10^6 km^2 to 20.3×10^6 km^2, than in the SMMR years, with the 18.0×10^6 km^2–19.1×10^6 km^2 range mentioned earlier (figure 4). The differences between the ESMR and SMMR instruments and the lack of an overlap period between the two records makes it difficult to be sure that the lower values during the SMMR years were real rather than instrumental, although it is interesting to note that in the case of the Arctic ice cover, the ESMR results showed generally lower rather than higher ice extent minima and yearly averages than the SMMR results (Parkinson & Cavalieri 1989). Independent of the instrument differences, the Southern Ocean maxima exhibited a monotonic decrease over the short ESMR record (figure 5–27 in Zwally *et al.* (1983*a*)), in sharp contrast to the SMMR results of figure 4. The decrease during the ESMR years was visible also in 12-month running means and continued, although not monotonically, for much of the remaining 1970s (Kukla & Gavin 1981), before reversing (Chiu 1983; Zwally *et al.* 1983*b*) and then levelling off during the SMMR years (figure 4).

A final comparison with the ESMR data concerns the occasional out-of-phase nature of the ice covers of the Ross and Weddell seas illustrated in the contrasting trends in the lengths of their ice seasons over the SMMR years (figure 7). A similar out-of-phase behaviour was found by Parkinson (1992) in a comparison of the distributions of monthly average ice coverage in the ESMR versus SMMR years. The ESMR years tended to show a more extensive ice coverage than the SMMR years in the Ross Sea but a less extensive ice coverage than the SMMR years in the Weddell Sea. Combining the two sets of results (Parkinson (1992) and figure 7 here), the suggestion from the short record is of out-of-phase back-and-forth fluctuations, not of consistent long-term trends.

The foregoing results show in a variety of forms some of the variability that occurred in Southern Ocean sea-ice distributions and extents over the 1970s and 1980s. Many case studies have been performed relating this variability to atmospheric and oceanographic factors (see examples mentioned previously, as well as reviews given by Parkinson (1989); Maslanik & Barry (1990); Gloersen *et al.* (1992)). However, although each case study provides information on the relationship of the sea-ice cover to the rest of the climate system, even when viewed together all the studies fall far short of providing a complete picture. Similarly, our knowledge of the variability of the Southern Ocean ice cover has greatly improved due to the roughly two decades of satellite coverage, but the existent satellite data fall far short of providing the full range of data desired. For instance, no satellite data have yet allowed reliable determinations of ice thickness or of melt ponding on the ice. Even for the aspects of the ice cover for which the satellite data have proven particularly useful, such as the overall ice distributions and extents described in this paper, the variability is such that surprises continue to arise, leaving considerable room for further increases in knowledge and understanding.

I thank the Royal Society for the opportunity to speak before them and to publish this paper in their *Transactions*. I also thank Jamila Saleh for her assistance during the generation of the figures and the Climate and Hydrological Systems Branch at NASA Headquarters for funding the research behind this work.

REFERENCES

Barry, R.G. & Chorley, R.J. 1985 *Atmosphere, weather and climate*, 4th edn. London: Methuen.

Carsey, F.D. 1980 Microwave observation of the Weddell polynya. *Mon. Weather Rev.* **108**, 2032–2044.

Cavalieri, D.J., Gloersen, P. & Campbell, W.J. 1984 Determination of sea ice parameters with the Nimbus 7 SMMR. *J. geophys. Res.* **89**, 5355–5369.

Chiu, L.S. 1983 Variation of Antarctic sea ice: An update. *Mon. Weather Rev.* **111**, 578–580.

Comiso, J.C. & Gordon, A.L. 1987 Recurring polynyas over the Cosmonaut Sea and the Maud Rise. *J. geophys. Res.* **92**, 2819–2833.

Cubasch, U. & Cess, R.D. 1990 Processes and modelling. In *Climate change: the IPCC scientific assessment* (ed. J. T. Houghton, G. J. Jenkins & J. J. Ephraums), pp. 69–91. Cambridge University Press.

Gloersen, P. & Barath, F.T. 1977 A scanning multichannel microwave radiometer for Nimbus-G and Seasat-A. *IEEE J. Oceanic Eng.* **OE-2**, 172–178.

Gloersen, P., Campbell, W.J., Cavalieri, D.J., Comiso, J.C., Parkinson, C.L. & Zwally, H.J. 1992 *Arctic and Antarctic sea ice, 1978–1987: satellite passive-microwave observations and analysis*. Washington, D.C.: National Aeronautics and Space Administration.

Gordon, A.L. 1981 Seasonality of Southern Ocean sea ice. *J. geophys. Res.* **86**, 4193–4197.

Grenfell, T.C. & Maykut, G.A. 1977 The optical properties of ice and snow in the Arctic Basin. *J. Glaciol.* **18**, 445–463.

Jacobs, S.S. & Comiso, J.C. 1989 Sea ice and oceanic processes on the Ross Sea continental shelf. *J. geophys. Res.* **94**, 18195–18211.

Killworth, P.D. 1983 Deep convection in the world ocean. *Rev. Geophys. Space Phys.* **21**, 1–26.

Kukla, G. & Gavin, J. 1981 Summer ice and carbon dioxide. *Science, Wash.* **214**, 497–503.

Maslanik, J.A. & Barry, R.G. 1990 Remote sensing in Antarctica and the Southern Ocean: applications and developments. *Antarctic Sci.* **2**, 105–121.

Maykut, G.A. 1982 Large-scale heat exchange and ice production in the central Arctic. *J. geophys. Res.* **87**, 7971–7984.

Parkinson, C.L. 1989 On the value of long-term satellite passive microwave data sets for sea ice/climate studies. *GeoJournal* **18**, 9–20.

Parkinson, C.L. 1992 Interannual variability of monthly Southern Ocean sea ice distributions. *J. geophys. Res.* **97**, 5349–5363.

Parkinson, C.L. & Cavalieri, D.J. 1989 Arctic sea ice 1973–1987: Seasonal, regional, and interannual variability. *J. geophys. Res.* **94**, 14499–14523.

Parkinson, C.L., Comiso, J.C., Zwally, H.J., Cavalieri, D.J., Gloersen, P. & Campbell, W.J. 1987 *Arctic sea ice, 1973–1976: satellite passive-microwave observations*. Washington, D.C.: National Aeronautics and Space Administration.

Warren, B.A. 1981 Deep circulation of the world ocean. In *Evolution of physical oceanography* (ed. B. A. Warren &

PHILOSOPHICAL TRANSACTIONS OF THE ROYAL SOCIETY B BIOLOGICAL SCIENCES

C. Wunsch), pp. 6–41. Cambridge, Massachusetts: Massachusetts Institute of Technology Press.
Zwally, H.J., Comiso, J.C., Parkinson, C.L., Campbell, W.J., Carsey, F.D. & Gloersen, P. 1983*a* *Antarctic sea ice, 1973–1976: satellite passive-microwave observations*. Washington, D.C.: National Aeronautics and Space Administration.
Zwally, H.J., Parkinson, C.L. & Comiso, J.C. 1983*b* Variability of Antarctic sea ice and changes in carbon dioxide. *Science, Wash.* **220**, 1005–1012.

Discussion

J. C. Moore (*British Antarctic Survey, Cambridge, U.K.*). Did Dr Parkinson observe any changes in sea-ice extent or character that can be associated with large-scale climate variability such as El Nino events?

C. L. Parkinson. I expect that eventually some firm relationships will be found between the sea-ice cover and El Nino events or other large-scale climate variabilities; but so far I know of no convincing studies in this regard. Part of the problem is the shortness of the existent records, as well as the continually evolving (and expanding) concept of what the El Nino phenomenon is.

B. Stonehouse (*Scott Polar Research Institute, Cambridge, U.K.*). I am interested in small polynyas, especially inshore polynyas in high latitudes that open early in spring and provide feeding opportunities for sea birds, seals and whales. Although persistent, they are often covered with nilas, which presumably reflects with low albedo. Examples are the coastal polynyas off Coats Land (Weddell Sea) and McMurdo Sound polynya (Ross Sea). Are these detectable on the scales on which Dr Parkinson is operating?

C. L. Parkinson. The satellite passive-microwave data generally have a horizontal resolution of 30–60 km, so that polynyas much smaller than that will only be detectable in a very approximate way, through the lower average ice concentration resulting from having a polynya in the field of view. The Coats Land polynya, however, is large enough to show up frequently on the December passive-microwave images as open water or very close to open water. The much larger Ross Sea polynya is often visible in both November and December in the satellite passive-microwave data, again as an open water feature. For detailed studies of polynyas with length scales considerably smaller than 30 km, higher resolution data, such as from the Advanced Very High Resolution Radiometer (AVHRR), would be preferable to the passive-microwave data. Regarding nilas: nilas has a microwave signature between that of open water and thicker ice, so that a polynya covered with nilas will show up in the microwave imagery as an area of reduced ice concentration and hence will be 'detectable' although with some ambiguity as to whether the region has a high concentration of nilas or a much lower concentration of thicker ice.

G. de Q. Robin. (*Scott Polar Research Institute, Cambridge, U.K.*). How have the algorithms used to convert ESMR and SMMR data to give percentage cover of sea ice changed between different satellites and different studies? Do the estimates of sea-ice cover change significantly with different algorithms?

C. L. Parkinson. The ESMR was a single-channel instrument, and the algorithm for calculating sea-ice concentrations (percent sea-ice coverage) from the ESMR data is essentially a linear algorithm, although with an adjustment for spatial differences in mean climatological temperatures. The SMMR was a ten-channel instrument, with many more possibilities for developing differing sea-ice algorithms and improving the accuracy over the accuracy possible with a single-channel sensor. The algorithm used for the images I showed today is called the SMMR Team Algorithm and is based on a polarization and gradient ratio using three of the ten SMMR channels. The estimated accuracy of the ESMR-derived ice concentrations is $\pm 15\%$, while that of the ice concentrations derived from the SMMR Team Algorithm is $\pm 7\%$. Unfortunately, there is no temporal overlap between the ESMR and SMMR data sets, so that differences between the ESMR and SMMR results for the same day cannot be obtained. Differences between the SMMR results using the Team Algorithm versus using one of the major alternative algorithms, termed the Bootstrap Algorithm, tend to be under 10% but occasionally rise as high as 25%.

PHILOSOPHICAL TRANSACTIONS OF THE ROYAL SOCIETY B BIOLOGICAL SCIENCES

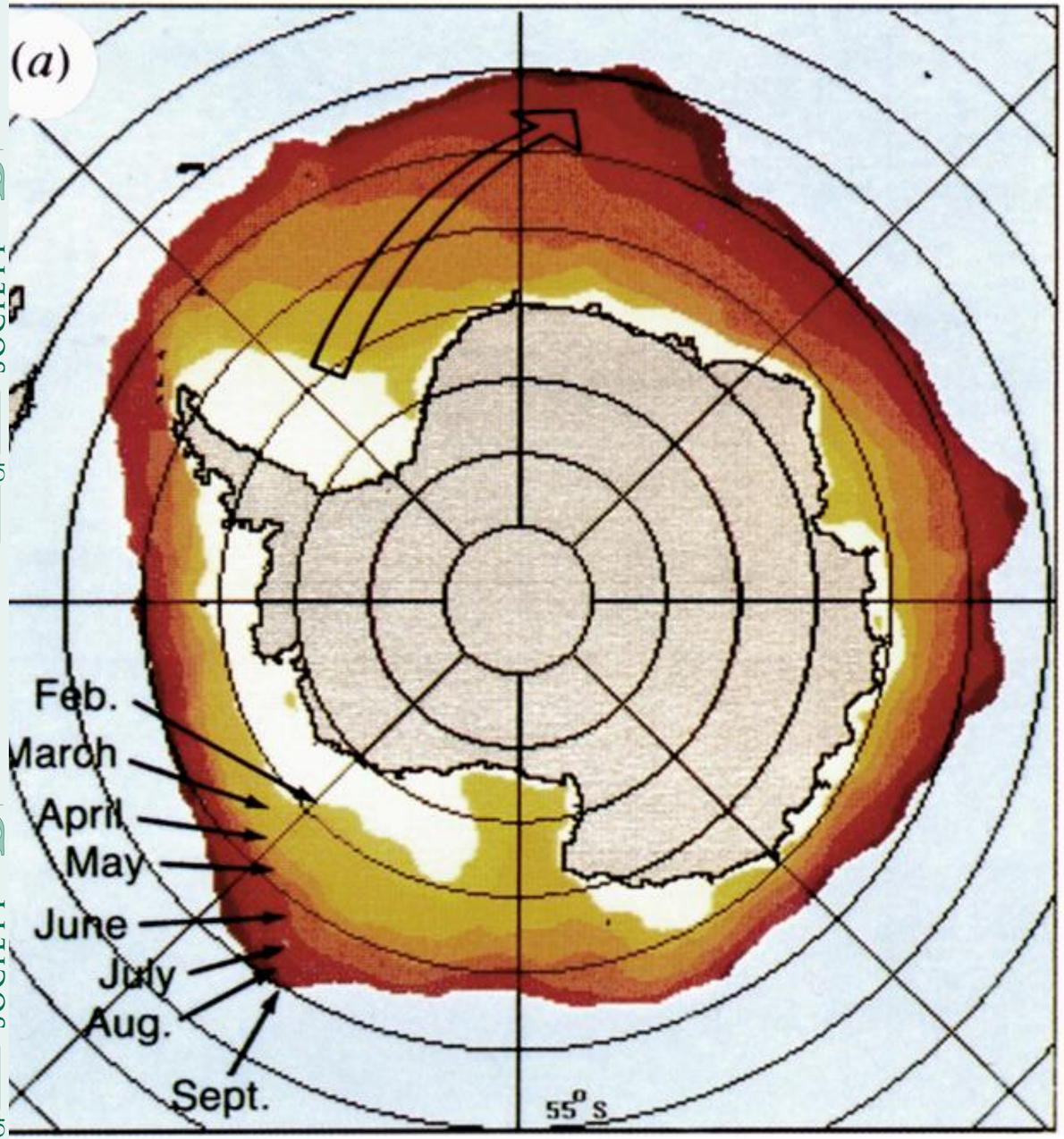

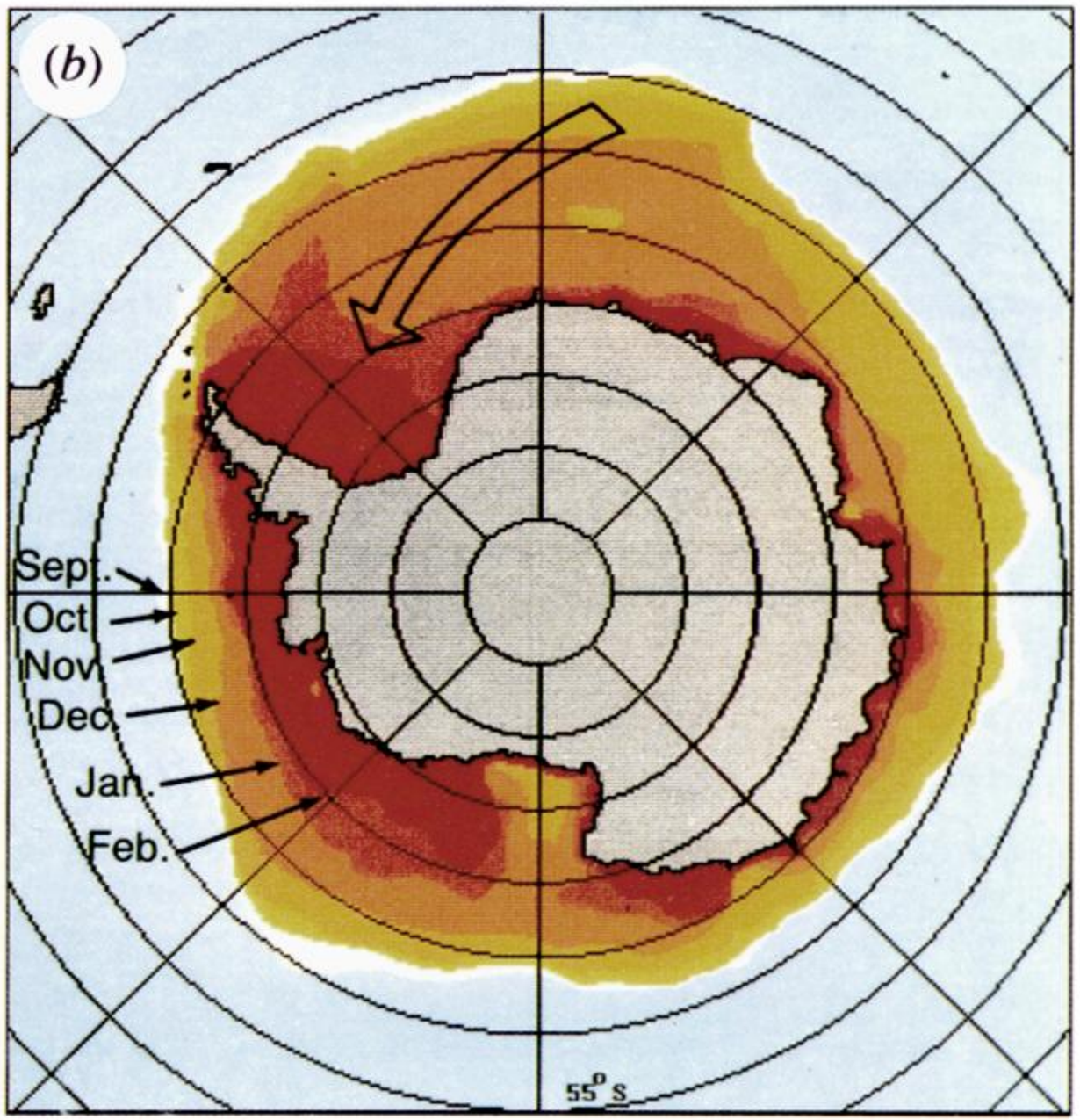

Figure 3. Average seasonal cycle of the monthly average spatial distributions of sea ice in the Southern Ocean over the period of the Nimbus 7 SMMR record, showing (*a*) the ice distributions during the growth period, February–September, and (*b*) the ice distributions during the decay period, September–February.

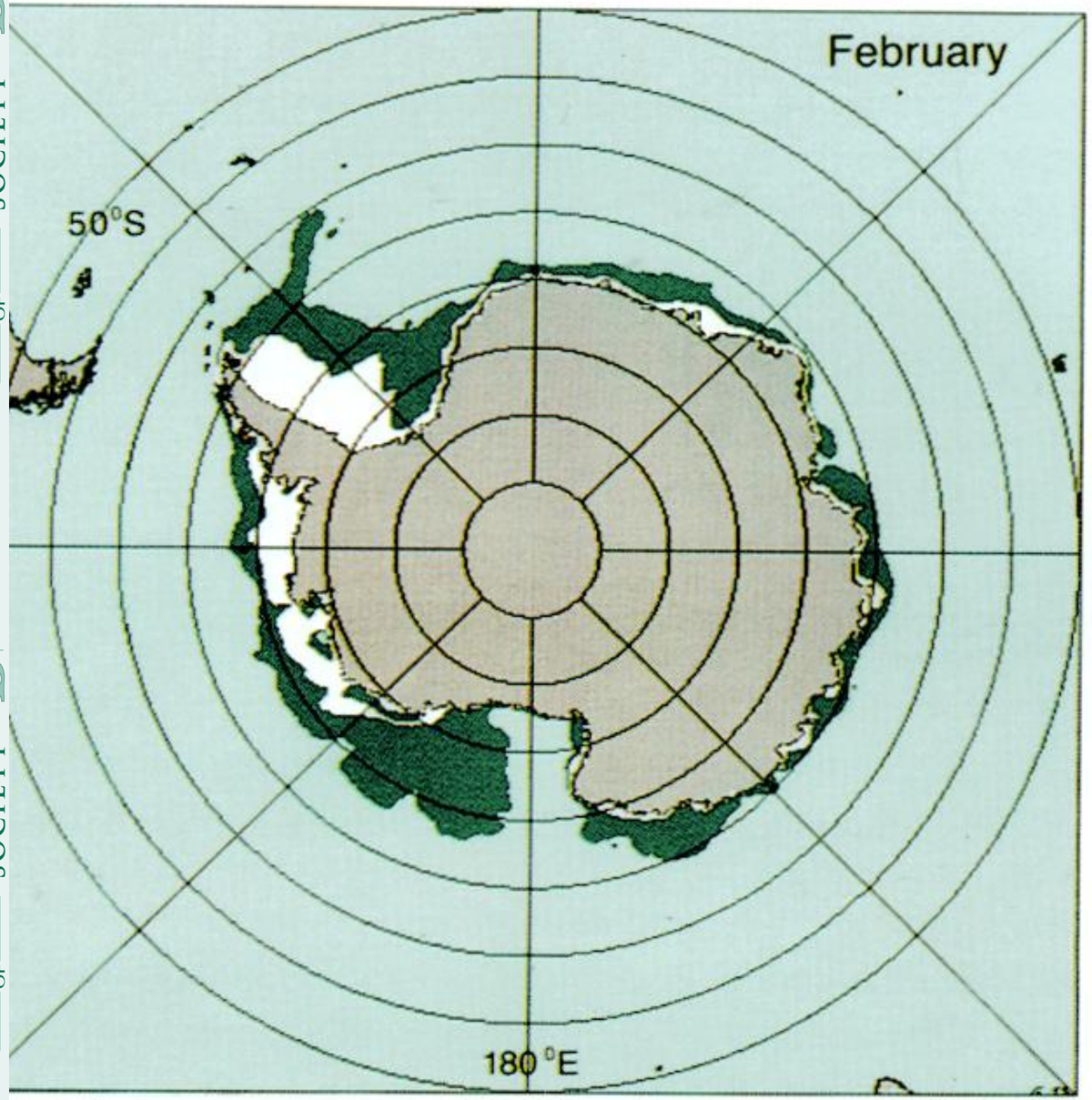

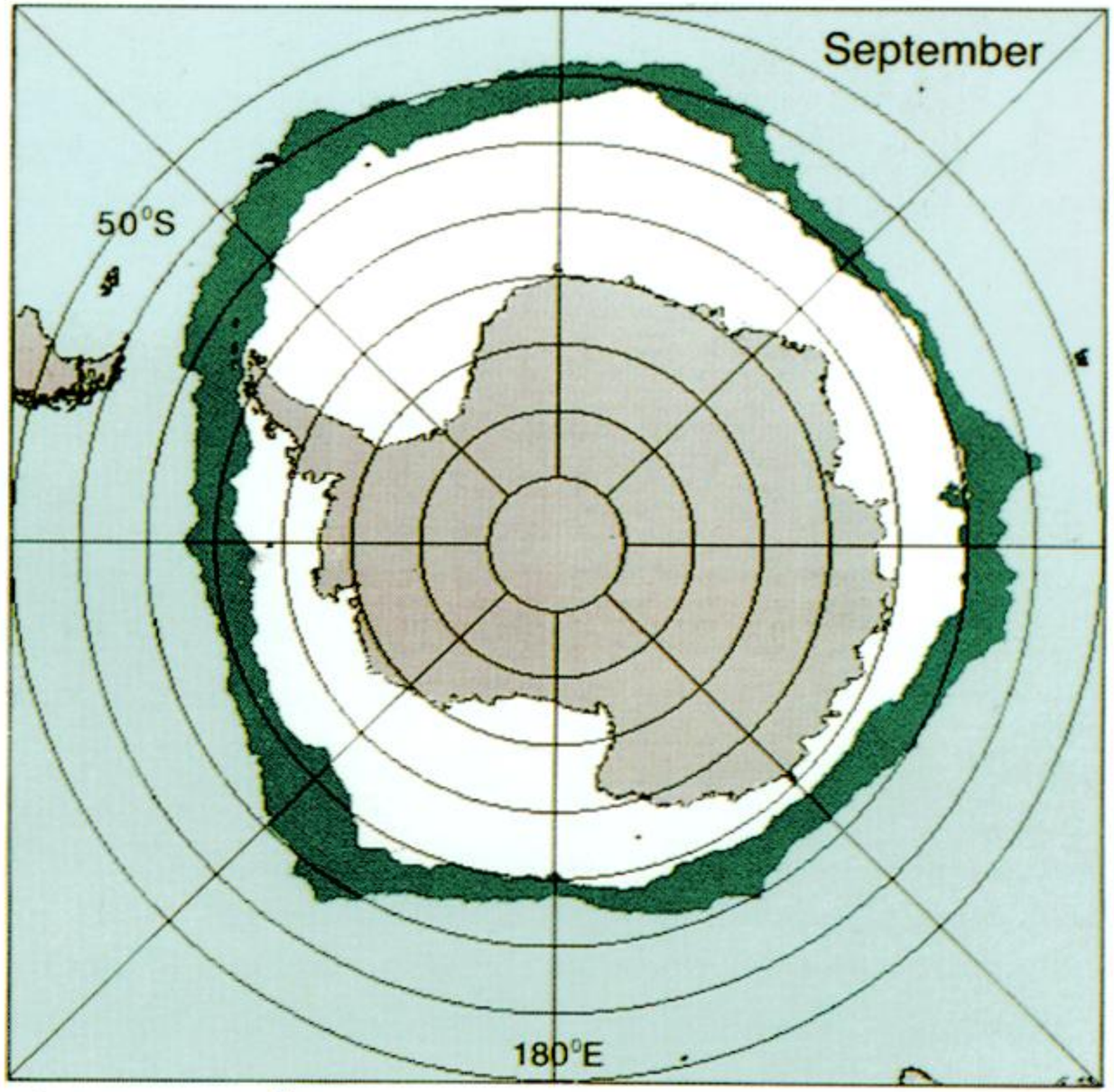

Figure 5. For description see opposite.

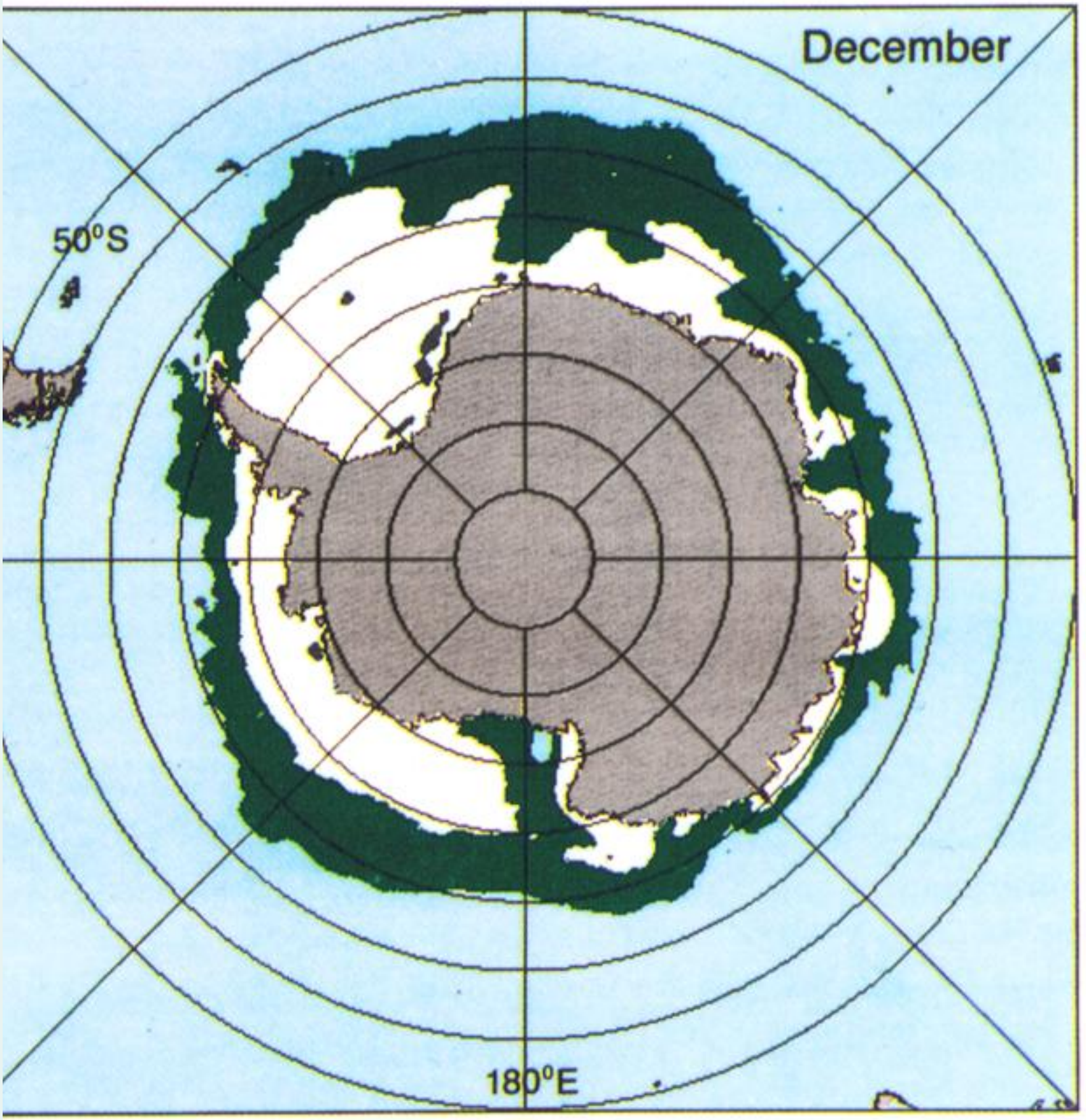

Figure 6. Same as figure 5 but for December.

PHILOSOPHICAL TRANSACTIONS OF THE ROYAL SOCIETY B BIOLOGICAL SCIENCES

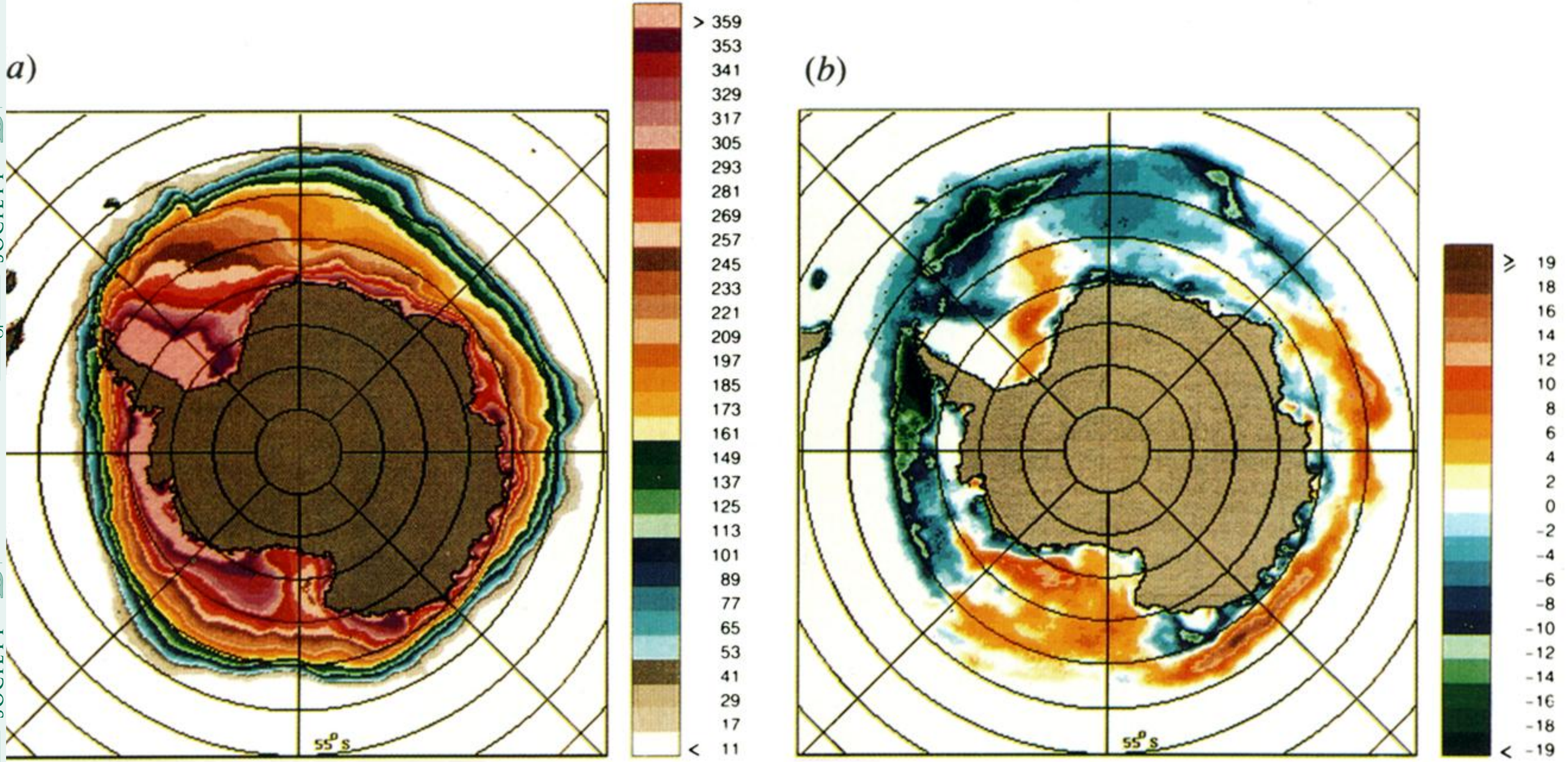

Figure 7. (*a*) Average length, in days, of the Southern Ocean sea-ice season, 1979–1986, as determined from the Nimbus 7 SMMR data, using an ice concentration cutoff of 15%. (*b*) Trends in the length of the Southern Ocean sea-ice season from 1979 to 1986, calculated as the slopes of the lines of least squares fit through the yearly values of the ice season lengths. The trends are given in units of days per year.